



Detection of chlorantraniliprole residues in tomato using field-deployable MIP photonic sensors

Ezequiel Rossi^{1,2} · Zahra Salahshoor² · Khanh-Van Ho^{3,4} · Chung-Ho Lin³ · Maria Ines Errea¹ · Maria M. Fidalgo²

Received: 24 October 2020 / Accepted: 25 January 2021 / Published online: 5 February 2021
© The Author(s), under exclusive licence to Springer-Verlag GmbH, AT part of Springer Nature 2021

Abstract

A photonic sensor based on inversed opal molecular imprinted polymer (MIP) film to detect the presence of chlorantraniliprole (CHL) residue in tomatoes was developed. Acrylic acid was polymerized in the presence of CHL inside the structure of a colloidal crystal, followed by etching of the colloids and CHL elution. Colloidal crystals and MIP films were characterized by scanning electron microscopy and FT-IR, confirming the inner structure and chemical structure of the material. MIP films supported on polymethylmethacrylate (PMMA) slides were incubated in aqueous solutions of the pesticide and in blended tomato samples. The MIP sensor displayed shifts of the peak wavelength of the reflection spectra in the visible range when incubated in CHL concentrations between 0.5 and 10 $\mu\text{g L}^{-1}$, while almost no peak displacement was observed for non-imprinted (NIP) films. Whole tomatoes were blended into a liquid and spiked with CHL; the sensor was able to detect CHL residues down to 0.5 $\mu\text{g kg}^{-1}$, significantly below the tolerance level established by the US Environmental Protection Agency of 1.4 mg kg^{-1} . Stable values were reached after about 30-min incubation in test samples. Control samples (unspiked processed tomatoes) produced peak shifts both in MIP and NIP films; however, this matrix effect did not affect the detection of CHL in the spiked samples. These promising results support the application of photonic MIP sensors as an economical and field-deployable screening tool for the detection of CHL in crops.

Keywords Molecularly imprinted polymer · Photonic sensor · Colloidal crystal · Pesticide detection · Chlorantraniliprole

Introduction

Chlorantraniliprole (CHL) is a persistent and mobile pesticide registered for use in several fruits and vegetable crops, with lifetimes over 200 days [1, 2]. It is assumed that pesticide concentration would be attenuated due to degradation, washing, leaching, etc., to a safe, acceptable level by the time the products reach the consumer [3]. CHL residue analyses are currently carried out by liquid chromatography (LC) coupled

with mass spectrometry (MS), with a limit of detection (LOD) between 1 and 20 $\mu\text{g kg}^{-1}$ depending on the analyzed crop [3]. Although the superior sensitivity of LC-MS makes it the preferred method for the analysis of contaminants in any type of sample, the cost of purchasing and maintaining an LC-MS system is non-negligible and it requires infrastructure typical of a chemical laboratory. The development of an economical and field-deployable method to screen for the presence of the pesticides prior to LC-MS measurement would result in significant savings in terms of time and economic resources. Since CHL was detected in only 13% of the fruit and vegetable samples analyzed in the USA in 2015 [3], a first screening of the samples will allow for only a small fraction of the tested crops to be sent to the laboratory, only those samples for which pesticide quantification is needed.

Molecularly imprinted polymers (MIPs) have been proposed as an alternative for this task. Molecular imprinting creates polymer materials that are able to selectively bind a target molecule on highly specific adsorption sites created during polymerization [4, 5]. In spite of the numerous reports in the literature about MIP technology in analysis and sensing

✉ Maria M. Fidalgo
fidalgom@missouri.edu

¹ Departamento de Ingeniería Química, Instituto Tecnológico de Buenos Aires, (C1106ACD) Buenos Aires, Argentina

² Department of Civil and Environmental Engineering, University of Missouri, Columbia, MO 65211, USA

³ Center for Agroforestry, School of Natural Resources, University of Missouri, Columbia, MO 65211, USA

⁴ Department of Food Technology, Can Tho University, Can Tho 90000, Vietnam

in several fields, commercial application of the technology is lagging due to knowledge gaps in real systems [4].

MIPs have been applied for food analysis mostly as solid-phase extraction (SPE) media coupled with an analytical instrument for quantification, such as HPLC-MS/MS. Besides, MIPs have been fabricated as materials that are capable to react to a variety of stimulus in order to obtain electrochemical, piezoelectric, photoluminescent, or UV-Vis spectroscopic biosensors [6, 7].

Inverse opal MIP films, which use colloidal crystals as templates for the morphology of their pore structure, have been reported for the fabrication of label-free photonic sensors [8, 9]. The methodology relies on the optical properties of the film, in particular the shift of the reflectance peak wavelength that occurs after target molecules are adsorbed [10, 11]. Pesticide detection by photonic MIPs was reported for several pesticides, including imidacloprid [12–14], atrazine [15, 16], 2,4-D [17], parathion [18], and methyl paraoxon [19]. However, the sensors were evaluated in either pure water, vegetable wash solutions, or diluted juice, which are unrealistic conditions for the intended application. To the best of our knowledge, there are no previous reports of a CHL sensor, or any pesticide sensor, tested under the standard sample processing conditions, as indicated by the Pesticide Data Program of the US Department of Agriculture (USDA PDP).

Herein we report the development of a MIP for the analysis of CHL residue in tomatoes, processed following USDA PDP guidelines. The proposed sensor comprises an optically active polymeric porous film that selectively captures the CHL molecules. The tomatoes were homogenized into a liquid and the MIP films were immersed into the samples. If present in the liquid, the pesticides were selectively adsorbed on the polymer. After a short equilibration time, the strip was rinsed with water and the reflectance spectrum was recorded. The maximum wavelength reflected was sensitive to the amount of rebound pesticide.

Experimental

Reagents and materials

Monodisperse silica particle were purchased from Pinfire - Gems & Colloids and characterized by electron microscopy in a FEI Quanta 600 FEG Environmental Scanning Electron Microscopy (ThermoFisher Scientific, Hillsboro, OR, USA). Acrylic acid (AA), azobisisobutyronitrile (AIBN), ethylene glycol dimethylacrylate (EGDMA), hydrofluoric acid (HF), and dimethylformamide (DMF) were purchase from Sigma-Aldrich (St. Louis, MO, USA). CHL, purity >95% was purchase from Key Organics (Bedford, MA, USA) while CHL analytical standard was obtained from Sigma-Aldrich (St. Louis, MO, USA). Ethanol 200 proof (anhydrous) was

purchase from Decon Laboratories Inc. (King of Prussia, PA, USA).

Glass microscope slides with dimensions $1 \times 13 \times 76$ mm were obtained from Fisher Scientific (Pittsburgh, PA, USA). Polymethylmethacrylate (PMMA) slides were purchased from ePlastic (San Diego, CA, USA) and cut into the same dimension as the glass slides. Ultra-pure water ($18.2 \text{ M}\Omega \cdot \text{cm}$ at $25 \text{ }^\circ\text{C}$) was used in all experiments and obtained from a Thermo Scientific™ Barnstead™ E-Pure™ Ultrapure Water Purification System (Waltham, MA, USA).

All reactants and solvents were purchased as reagent grade and used without further purification.

Molecular imprinted porous film fabrication

Silica particles (142.5 mg) were dispersed in 75 mL of ethanol. The suspension was stirred at 600 rpm for 1 h and then sonicated for another hour. This cycle was repeated three more times.

Colloidal crystals were prepared by vertical self-assembly of silica particles on a glass microscope slide acting as substrate, as described elsewhere [20–23]. Briefly, a cleaned slide was placed vertically into a 25-mL beaker containing the particle suspension. The system was left at rest at $50 \text{ }^\circ\text{C}$ for 24 h. As the ethanol is evaporated, the silica particles attach to both sides of the slide, forming colloidal crystals. PMMA slides were placed upon the colloidal crystal on both side of the glass slice and the three slides were firmly held together.

Polymerization solutions were prepared mixing 70.4 mg of CHL, 0.5 mL of DMF, 0.8 mL of AA, 0.55 mL of EGDMA, and 9 mg of AIBN. The optimum template-functional monomer-cross-linker molar ratio was chosen based on results from our previous studies; AA showed to high provide minimum resistance for the penetration of the solution and diffusion of the target due to its hydrophilicity, while the polymer was cross-linked to a degree that it produced a connected matrix but still allowed some flexibility for the chains to swell/shrink upon binding/eluting of the target [21–23]. The solution was sonicated in the dark for 15 min. One end of the assembly was partially dipped in the polymerization mixture; the liquid rose, driven by capillary forces, and occupied the empty spaces within the colloidal crystal. Polymerization was performed under UV light at wavelength of 365 nm for 5 h at room temperature. The glass slide and the silica particles were removed by submerging in 5% hydrofluoric acid bath. In order to remove the pesticide from the MIP, the sensors were washed in ethanol:acetic acid (9:1) solution for 15 min and repeated five times; the washing solution composition was selected based on our previously published results [21]. Because of the structural characteristic of the sensor, the hydrogen bonding is the main interaction between the polymer and the target that should be broken by the elution solvent in the desorption process. The capability of acetic acid:ethanol

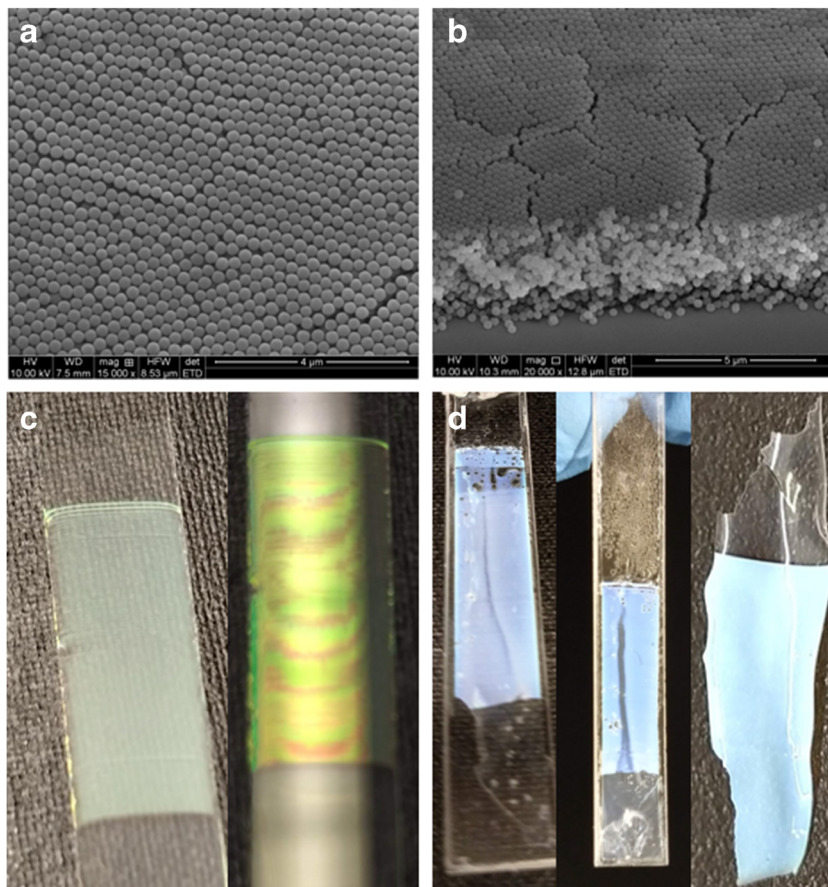
mixture to break this kind of intermolecular forces is well known. The 1:9 acetic acid:ethanol ratio was selected in order to protect the hydrogel from the acid. The desorption process was monitored by measurements of the reflectance spectra of the sensor after each wash (see Fig. S.1 in Supplementary Data) [21–23]. In the fabrication of the non-imprinted polymer (NIP), an analogous procedure was followed, but no CHL was added to the polymerization solution.

The polymeric films were analyzed by FT-IR in a Cary 660 spectrometer (Agilent Technologies, Santa Clara, CA, USA) between the wavelengths of 4000 and 400 cm^{-1} ; electron microscopy images were obtained in a FEI Quanta 600 FEG Environmental Scanning Electron Microscopy (ThermoFisher Scientific, Hillsboro, OR, USA).

Optical assays

In order to performed optical assays, MIP or NIP films were immersed in 25 mL of CHL aqueous solutions at different concentrations for 30 min. Reflectance spectra of the photonic polymeric sensors were measured over a wavelength range of 200–800 nm using a double-beam UV-visible spectrophotometer (Cary 60, Varian) with a Harrick Scientific's Specular Reflection Accessory (ERA-30G) at a fixed angle of 30°.

Fig. 1 **a** SEM image of colloidal crystal top layer; **b** SEM image of colloidal crystal showing cross section; **c** Photographs showing the photonic effect of some colloidal crystals; **d** Photographs showing the photonic effect of some molecular imprinted polymer films



Tomatoes were treated accordingly to the USDA PDP [3]. Briefly, tomatoes were washed under cold running water for 20 s and drained for at least 2 min. Any stem was remove using a clean dry knife, taking special attention to remove as little of the meat as possible. Then, the tomatoes were cut in 8 pieces and then homogenized using a home blender. The obtained juice was spiked with different concentrations of the pesticide and then the sensors were tested using the same procedure than for the aqueous solutions. All assays were performed in triplicate.

Analytical method

CHL concentration in aqueous solutions and tomato juices was determined using a Waters Alliance 2695 High Performance Liquid Chromatography (HPLC) system coupled with Waters TQ triple quadrupole tandem mass spectrometer (MS/MS; Water Alliance 2695, Water Co., Milford, MA, USA). The analyte was separated from the juice by a Phenomenex (Torrance, CA, USA) Kinetex C-18 reverse-phase column (100 mm \times 4.6 mm; 2.6- μm particle size). Mixtures of acetonitrile (A) and aqueous solution of 10 mM ammonium acetate and 0.1% formic acid (B), with a gradient conditions of 2% A, 2–80% A, 80–98% A, and 2% A at 0–

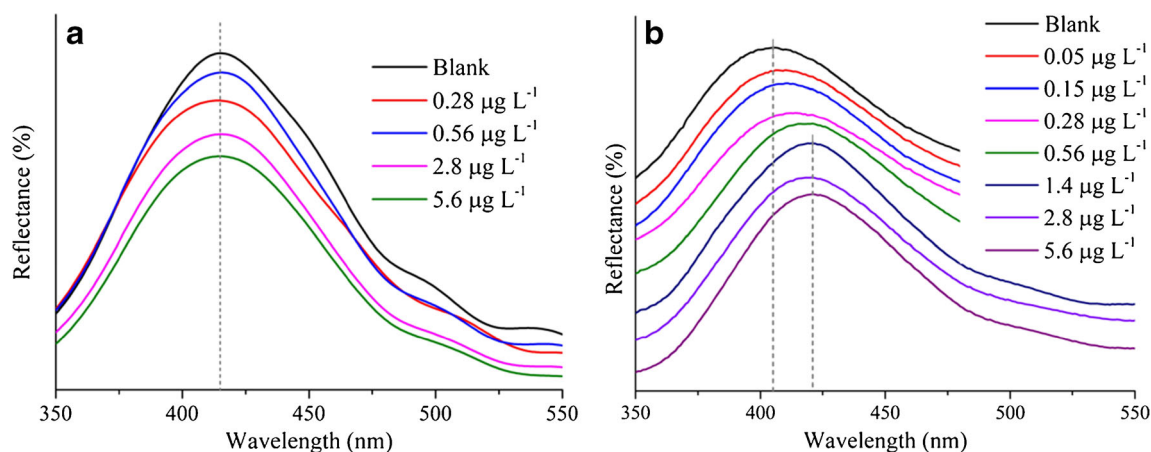


Fig. 2 Reflectance spectra of NIP (a) and MIP (b) after incubation at various concentration of CHL aqueous solution

0.5 min, 0.5–7 min, 7.0–9.0 min, and 9.0–15.0 min, respectively, were used as mobile phase with a flow rate of 0.5 mL/min. The ion source in the MS/MS system was electrospray ionization operated in the positive ion mode (ES+) with capillary voltage of 1500 V. The ionization sources and the desolvation temperature were programmed at 150 °C and 450 °C, respectively. The MS/MS system was operated in the multi-reaction monitoring mode with the optimized collision energy (MRM; $[M+H]^+ 484 \rightarrow 285$). Waters IntelliStart™ optimization software package was used to optimize the ionization energy, MRM transition ions (precursor and product ions), capillary and cone voltage, desolvation gas flow, and collision energy. The concentrations of CHL in samples were determined with a limit of detection (LOD) of 50 ng L^{-1} using a standard curve generated with an authentic standard (purity >95%, Sigma-Aldrich) at 9 concentrations (1, 5, 10, 25, 50, 100, 250, 500, and 1000 µg L^{-1}).

Results and discussion

Colloidal crystals and the photonic thin films were analyzed by SEM (Fig. 1 a, b and Fig. S.2 Supplementary Data). The nanoparticle size was measured using ImageJ software obtaining a diameter of 260 nm with a relative standard deviation of 5%, and the number of layers observed was between 12 and 15, what is in agreement with previously reported results [21–23]. SEM images of films after particle removal showed an open pore structure of spherical cavities derived from the templated particles, suggesting complete removal of the colloids.

The FT-IR spectrum of the sensor showed in the 2500–3500 cm^{-1} range the characteristic profile of the carboxylic acids due to the overlap of the stretching vibrations of $-\text{CH}_3$ and $-\text{CH}_2$ at 2918 and 2850 cm^{-1} and the stretching vibration of the O-H bond. Besides, in the broad peak at 1740 cm^{-1} are overlapped the C=O stretching vibration of the carboxyl

groups of PAA and the ester's carbonyl groups of EGDMA (Fig. S.3 Supplementary data).

The photonic effect (Fig. 1 c, d) observed on the colloidal crystal, as well as on the polymeric sensor, is a consequence of their uniformly ordered structure that produced optical interferences on the multiple light reflections. These interferences result on reflection patterns with peaks (λ_{max}) related to the structure of the porous film by the Bragg equation, as it was previously reported elsewhere [22, 24].

This photonic property can be used as a low-cost and simple approach for detection of the target [12, 15, 21, 25]. In a first place, preliminary studies in aqueous solution were carried out. The peak wavelength of the reflection spectra was correlated to the concentration of pesticide in the sample; as the concentration of CHL increased in the test solution, the peak is shifted to longer wavelengths. The inner pore structure of the MIP film, designed as an inverse opal, is deformed by the pesticide rebinding to the imprinted sites and produces a different optical response (Fig. 2). A noticeable difference between the behavior of MIPs and NIPs was observed. Contrary to MIP sensors, almost no peak displacements were observed for the NIP sensors under the same conditions

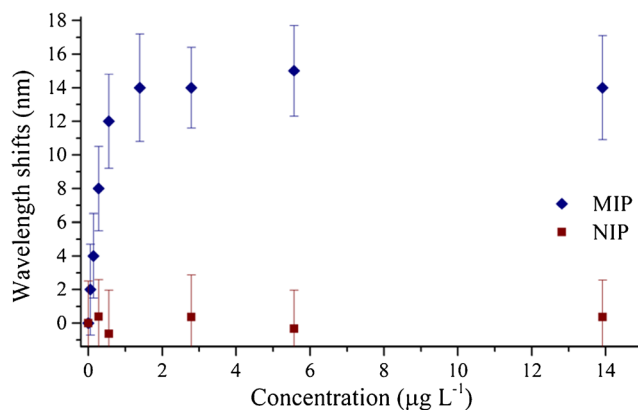


Fig. 3 Diffraction peak shift for MIP and NIP after incubation at various concentration of CHL aqueous solution (sample volume = 25 mL, incubation time = 30 min)

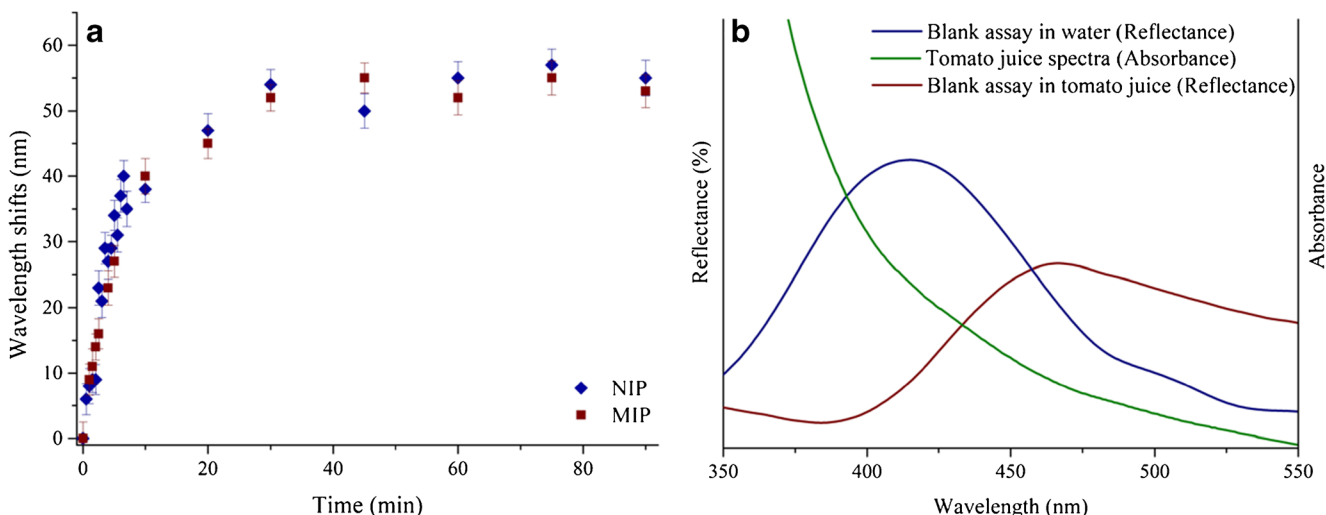


Fig. 4 a Diffraction peak shift for MIP and NIP after incubation in tomato juice at different times (sample volume = 25 mL); b NIP reflectance spectra before and after being in touch with tomato juice overlapped with the absorption spectra of tomato juice

(Fig. 3). The limit of detection was $0.5 \mu\text{g L}^{-1}$, below the tolerance level set by USEPA of 1.4 mg L^{-1} [3], calculated as concentration associated with three times the standard deviation of 10 independent measurement of the procedural blank (3σ criterion) (standard deviation measured on wavelength = 2.5 nm).

In order to test the applicability of the developed method, the MIPs were used to analyze the presence of CHL in homogenized tomato samples treated according to the USDA PDP protocol. The election of this vegetable was made considering that, according to the Pesticide Data Program made by the Department of Agriculture of the USA, tomato was one of the crops with higher incidence of CHL [3].

Blank experiments were carried out in order to analyze the effect of the tomato matrix in the results by immersing NIP and MIP sensors in the tomato juice without addition of the pesticides. As it is shown in Fig. 4a, in both MIP and NIP sensors, the diffraction peak shift increased with time until

reaching a stable value after about 30 min. Besides, the reflectance spectra after being in touch with tomato juice appear shifted and deformed (Fig. 4 b). These results were consistent with the present of an absorption band on the spectra of tomato juice in the region that the sensors reflect the light (Fig. 4 b). If the pigment that is responsible of the tomato absorption band remained in the surface of the sensor after washing, it may cause the deformation observed in the reflectance spectra.

However, when MIPs and NIPs were immersed in the doped samples, the shift observed in the diffraction peak of MIP sensor was consistently higher than that of NIP sensor at each concentration tested. Furthermore, as it was observed in the aqueous solutions, MIPs exposed to increasing concentration of CHL exhibited peaks that gradually shifted to longer wavelengths (Fig. 5 a). As it can be observed in Fig. 5 b, the difference between MIP and NIP on the diffraction peak shift against CHL concentration in tomato juice resemble to that obtained in aqueous solution. Therefore, the tomato matrix did

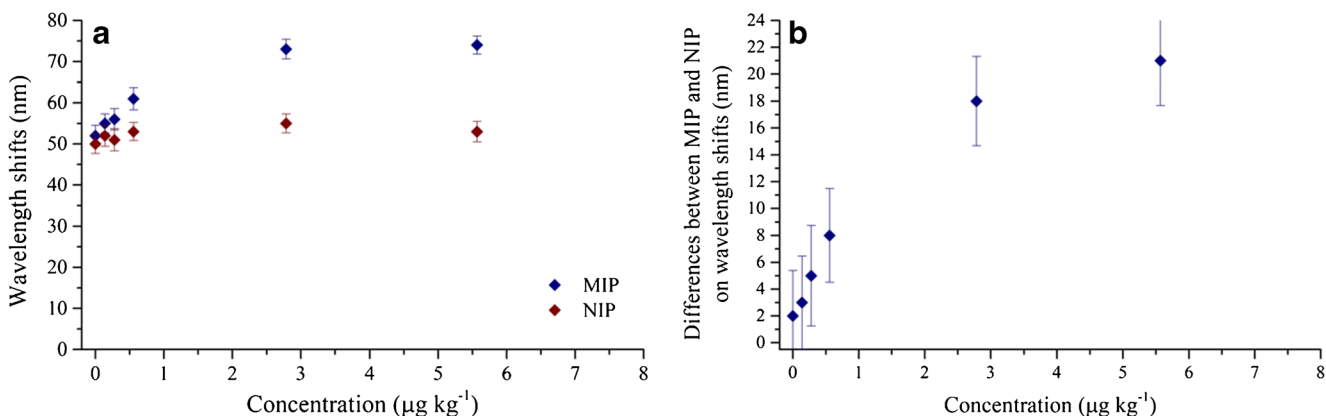


Fig. 5 a Diffraction peak shift for MIP and NIP after incubation in tomato juice with various concentration of CHL (sample volume = 25 mL, incubation time = 30 min); b Differences between MIP and NIP diffraction peak shifts at each tested concentration

not affect the detection of the pesticide, which could be detected with a LOD of $0.5 \mu\text{g L}^{-1}$, well below the tolerance level established by the USEPA of 1.4 mg L^{-1} .

Conclusion

The photonic MIP films were able to detect CHL residue in tomatoes processed according to the USDA PDP, with a LOD of $0.5 \mu\text{g L}^{-1}$. The sensor is a user-friendly, economical, and field-deployable method. The limit of detection was below the tolerance level established by the USEPA and, even more, lower than that informed by the USDA PDP for tomatoes using HPLC/MS in specialized laboratories. Due to its advantageous characteristics, these sensors could be a great improvement in the analytical methods for the determination of residual pesticide concentrations in food, particularly as a first screening tool in the field.

The absorption band of the tomato matrix observed in the area of reflection of the MIP reveals the problems associated with the use of optical sensors in complex matrices and highlights the importance of applied research conducted under realistic conditions to promote the translation of these technologies to commercial applications.

Supplementary Information The online version contains supplementary material available at <https://doi.org/10.1007/s00604-021-04731-2>.

Acknowledgements E. Rossi would like to acknowledge CONICET for his fellowship.

Funding The authors are grateful to the Instituto Tecnológico de Buenos Aires (ITBA) and the University of Missouri College of Engineering for financial support.

Declarations

Conflict of interest The authors declare that they have no conflict of interest.

References

- Vijayasree V, Bai H, Beevi SN, Mathew TB, Kumar V, George T, Xavier G (2013) Persistence and effects of processing on reduction of chlorantraniliprole residues on cowpea fruits. *Bull Environ Contam Toxicol* 90(4):494–498
- O'Connell DW, Birkinshaw C, O'Dwyer TF (2008) Heavy metal adsorbents prepared from the modification of cellulose: a review. *Bioresour Technol* 99(15):6709–6724
- USDA (2015) Pesticide data program, annual summary. Agricultural Department, United States
- Chiappini A, Pasquardini L, Bossi AM (2020) Molecular imprinted polymers coupled to photonic structures in biosensors: the state of art. *Sensors* 20(18):5069. <https://doi.org/10.3390/s20185069>
- Usman L, Adnan M, Muhammad Z, Ghulam M, Akhtar H (2020) Nanostructured molecularly imprinted photonic polymers for sensing applications. *Curr Nanosci* 16(4):495–503. <https://doi.org/10.2174/1573413715666190206144415>
- Ashley J, Shahbazi M-A, Kant K, Chidambara VA, Wolff A, Bang DD, Sun Y (2017) Molecularly imprinted polymers for sample preparation and biosensing in food analysis: progress and perspectives. *Biosens Bioelectron* 91:606–615. <https://doi.org/10.1016/j.bios.2017.01.018>
- Yan X, Li H, Su X (2018) Review of optical sensors for pesticides. *TrAC Trends Anal Chem* 103:1–20. <https://doi.org/10.1016/j.trac.2018.03.004>
- Chiappini A, Tran LTN, Trejo-García PM, Zur L, Lukowiak A, Ferrari M, Righini GC (2020) Photonic crystal stimuli-responsive chromatic sensors: a short review. *Micromachines* 11(3):290. <https://doi.org/10.3390/mi11030290>
- Fathi F, Rashidi M-R, Pakchin PS, Ahmadi-Kandjani S, Nikniazi A (2021) Photonic crystal based biosensors: emerging inverse opals for biomarker detection. *Talanta* 221:121615. <https://doi.org/10.1016/j.talanta.2020.121615>
- Lin Z-z, Li L, G-y F, Z-z L, A-h P, Z-y H (2020) Molecularly imprinted polymer-based photonic crystal sensor array for the discrimination of sulfonamides. *Anal Chim Acta* 1101:32–40. <https://doi.org/10.1016/j.aca.2019.12.032>
- Han S, Jin Y, Su L, Chu H, Zhang W (2020) A two-dimensional molecularly imprinted photonic crystal sensor for highly efficient tetracycline detection. *Anal Methods* 12(10):1374–1379. <https://doi.org/10.1039/D0AY00110D>
- Wang X, Mu Z, Liu R, Pu Y, Yin L (2013) Molecular imprinted photonic crystal hydrogels for the rapid and label-free detection of imidacloprid. *Food Chem* 141(4):3947–3953. <https://doi.org/10.1016/j.foodchem.2013.06.024>
- Farooq S, Nie J, Cheng Y, Yan Z, Bacha SAS, Zhang J, Nahiyoon RA, Hussain Q (2019) Synthesis of core-shell magnetic molecularly imprinted polymer for the selective determination of imidacloprid in apple samples. *J Sep Sci* 42(14):2455–2465. <https://doi.org/10.1002/jssc.201900221>
- Kumar N, Narayanan N, Gupta S (2018) Application of magnetic molecularly imprinted polymers for extraction of imidacloprid from eggplant and honey. *Food Chem* 255:81–88. <https://doi.org/10.1016/j.foodchem.2018.02.061>
- Wu Z, C-a T, Lin C, Shen D, Li G (2008) Label-free colorimetric detection of trace atrazine in aqueous solution by using molecularly imprinted photonic polymers. *Chem Eur J* 14(36):11358–11368. <https://doi.org/10.1002/chem.200801250>
- Yang JC, Park JY (2016) Polymeric colloidal nanostructures fabricated via highly controlled convective assembly and their use for molecular imprinting. *ACS Appl Mater Interfaces* 8(11):7381–7389. <https://doi.org/10.1021/acsami.6b00375>
- Aya GA, Yang JC, Hong SW, Park JY (2019) Replicated pattern formation and recognition properties of 2,4-dichlorophenoxyacetic acid-imprinted polymers using colloidal silica Array molds. *Polymers* 11(8):1332
- Zhang X, Cui Y, Bai J, Sun Z, Ning B, Li S, Wang J, Peng Y, Gao Z (2017) Novel biomimic crystalline colloidal array for fast detection of trace parathion. *ACS Sensors* 2(7):1013–1019. <https://doi.org/10.1021/acssensors.7b00281>
- Walker JP, Kimble KW, Asher SA (2007) Photonic crystal sensor for organophosphate nerve agents utilizing the organophosphorus hydrolase enzyme. *Anal Bioanal Chem* 389(7):2115–2124. <https://doi.org/10.1007/s00216-007-1599-y>
- Jiang P, Bertone JF, Hwang KS, Colvin VL (1999) Single-crystal colloidal multilayers of controlled thickness. *Chem Mater* 11(8):2132–2140. <https://doi.org/10.1021/cm990080+>
- Kadhem A, Xiang S, Nagel S, Lin C-H, Fidalgo de Cortalezzi M (2018) Photonic molecularly imprinted polymer film for the detection of testosterone in aqueous samples. *Polymers* 10(4):349

22. Dai J, Vu D, Nagel S, Lin C-H, Fidalgo de Cortalezzi M (2017) Colloidal crystal templated molecular imprinted polymer for the detection of 2-butoxyethanol in water contaminated by hydraulic fracturing. *Microchim Acta* 185(1):32. <https://doi.org/10.1007/s00604-017-2590-8>
23. Dai J, Dong X, Fidalgo de Cortalezzi M (2017) Molecularly imprinted polymers labeled with amino-functionalized carbon dots for fluorescent determination of 2,4-dinitrotoluene. *Microchim Acta* 184(5):1369–1377. <https://doi.org/10.1007/s00604-017-2123-5>
24. Griffete N, Frederich H, Maître A, Ravaine S, Chehimi MM, Mangeney C (2012) Inverse opals of molecularly imprinted hydrogels for the detection of bisphenol A and pH sensing. *Langmuir* 28(1):1005–1012. <https://doi.org/10.1021/la202840y>
25. Wang L-Q, Lin F-Y, Yu L-P (2012) A molecularly imprinted photonic polymer sensor with high selectivity for tetracyclines analysis in food. *Analyst* 137(15):3502–3509. <https://doi.org/10.1039/C2AN35460H>

Publisher's note Springer Nature remains neutral with regard to jurisdictional claims in published maps and institutional affiliations.